Low-intensity pulsed ultrasound accelerates diabetic wound healing by ADSC-derived exosomes via promoting the uptake of exosomes and enhancing angiogenesis

FANGLU ZHONG[1*], SHENG CAO[1*], LI YANG[2], JUNBI LIU[1], BIN GUI[1], HAO WANG[1], NAN JIANG[1], QING ZHOU[1] and QING DENG[1]

[1]Department of Ultrasound, Renmin Hospital of Wuhan University, Wuhan, Hubei 430060; [2]Department of Ultrasound, General Hospital of Central Theater Command, Wuhan, Hubei 430070, P.R. China

Received June 30, 2023; Accepted November 15, 2023

DOI: 10.3892/ijmm.2024.5347

Abstract. Diabetic wounds remain a great challenge for clinicians globally as a lack of effective radical treatment often results in poor prognosis. Exosomes derived from adipose-derived stem cells (ADSC-Exos) have been explored as an appealing nanodrug delivery system in the treatment of diabetic wounds. However, the short half-life and low utilization efficiency of exosomes limit their therapeutic effects. Low-intensity pulsed ultrasound (LIPUS) provides a non-invasive mechanical stimulus to cells and exerts a number of biological effects such as cavitation and thermal effects. In the present study, whether LIPUS could enhance ADSC-Exo-mediated diabetic wound repair was investigated and its possible mechanism of action was explored. After isolation and characterization, ADSC-Exos were injected into mice with diabetic wounds, then the mice were exposed to LIPUS irradiation. The control mice were subcutaneously injected with PBS. Wound healing assays, laser Doppler perfusion, Masson's staining and angiogenesis assays were used to assess treatment efficiency. Then, ADSC-Exos were cocultured with human umbilical vein endothelial cells (HUVECs), and the proliferation, migration and tube formation of HUVECs were assessed. Moreover, the cellular uptake of ADSC-Exos *in vitro* and *in vivo* was assessed to explore the synergistic mechanisms underlying the effects of LIPUS. The *in vivo* results demonstrated that LIPUS increased the uptake of exosomes and prolonged the residence of exosomes in the wound area, thus enhancing angiogenesis and accelerating wound repair in diabetic mice. The *in vitro* results further confirmed that LIPUS enhanced the uptake efficiency of ADSC-Exos by 10.93-fold and significantly increased the proliferation, migration and tubular formation of HUVECs. Therefore, the present study indicates that LIPUS is a promising strategy to improve the therapeutic effects of ADSC-Exos in diabetic wounds by promoting the cellular uptake of exosomes and enhancing angiogenesis.

Correspondence to: Dr Qing Zhou or Dr Qing Deng, Department of Ultrasound, Renmin Hospital of Wuhan University, 238 Jiefang Road, Wuchang, Wuhan, Hubei 430060, P.R. China
E-mail: qingzhou128@163.com
E-mail: wudadq@163.com

*Contributed equally

Abbreviations: DFUs, diabetic foot ulcerations; ADSCs, adipose-derived stem cells; ADSC-Exos, exosomes derived from ADSCs; LIPUS, low-intensity pulsed ultrasound; HUVECs, human umbilical vein endothelial cells; TEM, transmission electron microscopy; DAPI, 4,6-diamidino-2-phenylindole; H&E, hematoxylin and eosin; α-SMA, α-smooth muscle actin; CCK-8, Cell Counting Kit-8; MPU, mean perfusion unit

Key words: low-intensity pulsed ultrasound, exosomes, stem cell, diabetic wound healing

Introduction

Chronic diabetic wounds are a global healthcare challenge. It is estimated that impaired healing of diabetic wounds affects ~20% of all patients with diabetes mellitus worldwide (1). Diabetic foot ulcers (DFUs) represent the most severe form of diabetic wounds, and have a number of serious complications, including amputation, poor quality of life and life-threatening infections (2). Diabetic wounds often take a long time to heal and may recur after healing. These wounds consume a significant amount of medical resources (3) and globally, 30% of diabetes-related treatment costs are spent on DFUs (4). These consequences have serious public health and clinical implications such as poor prognosis and dissatisfaction with clinical outcomes (5). It is estimated that 15% of diabetic patients in the USA will suffer from DFUs in their lifetime (6). Due to 9.4% of the global population suffering from diabetes, the number of individuals receiving DFU treatment may be vast (6). Chronic diabetic wounds cause great pain for patients and increase the financial burden on the families of the patient.

Debridement is the main clinical treatment for DFUs (2). For smaller wounds, debridement can clear the necrotic tissue, close the wound early and avoid serious clinical outcomes, such as amputation. However, due to vascular insufficiency, peripheral neuropathy, immunosuppression and critical

colonization/infection, it is difficult for debridement to achieve the desired effect (6). Normal wound healing involves the following four phases: Hemostasis/coagulation, inflammatory, proliferative and maturation/remodeling phase (7). In diabetes, these physiological processes are disturbed (8). The mechanisms that affect diabetic wound healing are complicated as hyperglycemia seriously hinders the physiological process of normal wound healing, and impaired angiogenesis is one of the key factors (9-11). Stem cell-based angiogenesis is an appealing approach for the treatment of chronic non-healing wounds. It has been reported that stem cells can enhance wound healing and tissue regeneration through the regulation of immune responses and promotion of angiogenesis (12,13). However, due to the low survival rate of stem cells in diabetic wounds, it is difficult to achieve satisfactory results.

A growing body of evidence has demonstrated the therapeutic potential of exosomes derived from adipose-derived stem cells (ADSC-Exos) for repairing diabetic wounds (14-16). Studies have also shown that ADSC-Exos have similar therapeutic functions to ADSCs, both of which can effectively promote the formation of new blood vessels and restore skin morphology and function (17,18). Compared with ADSC therapy, ADSC-Exos have certain unique advantages, including higher stability, better storage and minimal immune rejection (19). Thus, the use of exosomes may be a promising approach for developing a cell-free alternative to stem cell therapy. However, due to the low yield of exosomes and their relatively short half-life *in vivo*, the clinical applications of ADSC-Exos still face challenges (20). It is difficult to significantly increase the yield of ADSC-Exos under the current established protocols. The number of exosomes produced by exocytosis in the physiological state of cells is limited, while the contents and functions of exosomes produced by molecular interference remain to be determined. However, improving the utilization efficiency of ADSC-Exos is currently a more realistic approach in improving efficacy. Increasing exosome uptake by target cells through external stimulation before metabolic clearance may be an effective method in improving the utilization efficiency of ADSC-Exos.

Low-intensity pulsed ultrasound (LIPUS) is a type of specific physical energy that is delivered at a low intensity (<3 W/cm^2) and outputs in the mode of pulsed waves. LIPUS has minimal thermal effects while maintaining the transmission of acoustic energy to the target tissue. LIPUS provides a non-invasive localized mechanical stimulus to cells and has significant biological effects such as promoting intracellular signal transduction, enhancing cell proliferation and inhibiting autophagy (21). In the last 10 years, LIPUS stimulation has emerged as a promising technique in many therapeutic applications, such as the healing of fresh fractures, soft tissue regeneration and nerve regulation (22-24). Certain studies have indicated that LIPUS may participate in cell proliferation, differentiation and apoptosis by regulating intracellular signals (25-27). However, whether LIPUS plays a significant role in promoting the uptake of exosomes by target cells and thus improving the utilization efficiency of exosomes remains unknown.

In the present study, we hypothesized that LIPUS could effectively enhance the uptake of ADSC-Exos *in vitro* and *in vivo*, thus markedly improving angiogenesis and promoting diabetic wound healing (a schematic illustration of this is shown in Fig. 1). The aim of the present study was to obtain preliminary evidence of a link between LIPUS and exosome uptake and to explore how LIPUS enhances therapeutic angiogenesis of stem cell-derived exosomes to repair diabetic wounds.

Materials and methods

Isolation and identification of ADSCs. ADSCs were isolated from the inguinal fat pads of male SD rats as previously described (28). Briefly, 10 rats were raised in an SPF environment (temperature, 27˚C; humidity, 60-70%; noise, <60 dB) until they were 5 weeks old (110.0±3.0 g). Then, these rats were euthanized by cervical dislocation, bilateral groin adipose tissue was obtained under sterile conditions and other tissue such as blood vessels and blood clots were removed. The adipose tissue was crushed with scissors and digested at 37˚C and 120 rpm/min for 60 min in a constant temperature shaking table. The sample was then centrifuged at 285 x g at 4˚C for 10 min and the supernatant discarded. The cells were re-suspended and maintained in Dulbecco's modified Eagle's medium (HyClone; Cytiva) supplemented with 10% fetal bovine serum (FBS; HyClone; Cytiva) and incubated at 37˚C in a humidified atmosphere with 5% CO_2.

ADSCs in the third passage were used for cell identification. For this, cell morphology was observed with a light microscope (Olympus Corporation). To identify the multilineage differentiation potential of ADSCs, osteogenic and adipogenic differentiation medium kits (Cyagen Biosciences, Inc.) were used for cell culture and staining, according to the manufacturer's instructions. Surface antigen expression of ADSCs were also analyzed by flow cytometry. Briefly, 3x10^5 cells were harvested following treatment with 0.25% trypsin-EDTA and washing twice with PBS. The cells were then incubated for 30 min at 4˚C with a specific monoclonal antibody conjugated to either fluorescein isothiocyanate or phycoerythrin in 200 μl PBS for 30 min in the dark at 4˚C. Flow cytometry (FACS Calibur; BD Biosciences) was then performed to determine the expression of specific cell surface antigens, and FlowJo 10.8.1 (FlowJo LLC) software was used for analysis. Antibodies specific for CD29 (cat. no. A14886; eBioscience; Thermo Fisher Scientific, Inc.), CD34 and CD90 (cat. nos. MA5-17832 and A14726; eBioscience; Thermo Fisher Scientific, Inc.) were used for the identification of ADSCs.

Extraction and characterization of ADSC-Exos. ADSCs in the third passage were used for exosome extraction. Upon reaching 80-90% confluency, the ADSCs were washed with PBS and cultured in fresh serum-free medium before exosome extraction. After 48 h of culture, the supernatants were collected. ADSC-Exos were extracted by differential ultracentrifugation as described previously, with some modifications (29). Briefly, the supernatant was centrifuged at 4,000 x g for 15 min to remove the cells and then centrifuged at 10,000 x g for 30 min to remove the cell debris. Exosomes were pelleted by ultracentrifugation at 100,000 x g for 70 min at 4˚C to eliminate contaminating proteins. The obtained ADSC-Exos were resuspended in 1X PBS and stored at -80˚C for future use.

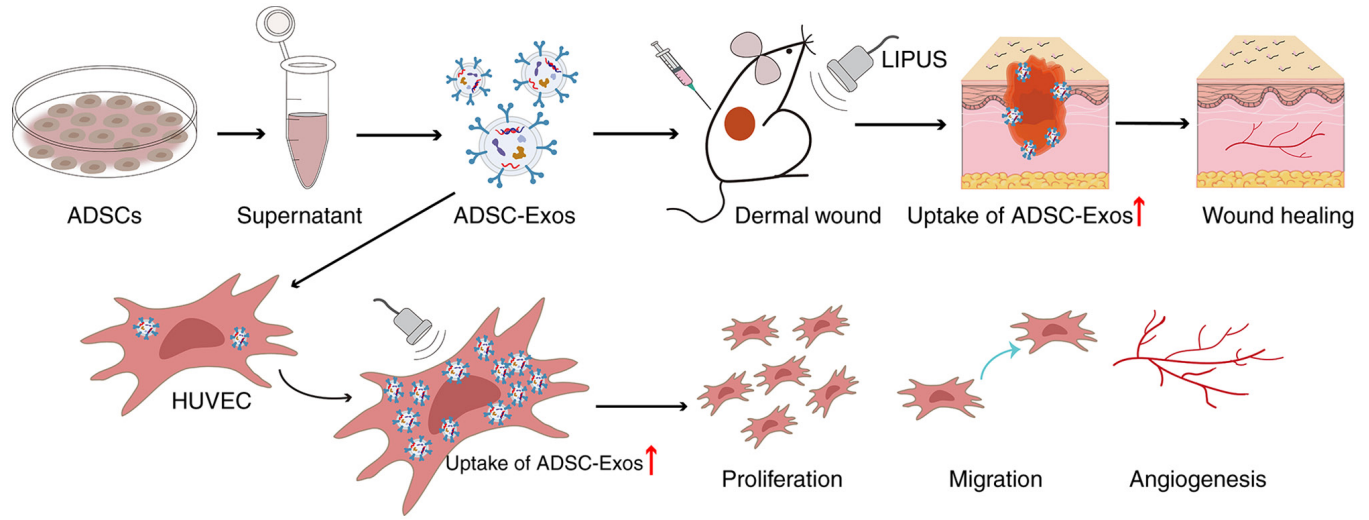

Figure 1. Schematic of the present study. LIPUS accelerates ADSC-Exos-mediated diabetic wound healing by promoting the uptake of exosomes and enhancing angiogenesis. ADSCs, adipose-derived stem cells; ADSC-Exos, exosomes derived from ADSCs; LIPUS, low-intensity pulsed ultrasound; HUVEC, human umbilical vein endothelial cell.

The morphology of the ADSC-Exos was verified by transmission electron microscopy (TEM; HT7700; Hitachi, Ltd.). For negative staining, the samples were incubated with 2% phosphotungstic acid solution for 10 min at room temperature. Nanoparticle tracking analysis was performed at room temperature using a ZetaView PMX 110 (Particle Metrix GmbH) to determine the size distribution and concentration of the exosomes in each sample. Each sample was diluted to $1x10^5$/ml with PBS, and all experiments were repeated three times. The expression levels of the exosomal markers, CD9 and tumor susceptibility gene 101 (Tsg101) (1:1,000; cat. nos. 20597-1-AP and 28283-1-AP, respectively; Proteintech, Group, Inc.), were analyzed by western blotting. Calnexin (1:1,000; 10427-2-AP; Proteintech, Group, Inc.), a specific protein of the cellar endoplasmic reticulum, was used as a negative control. After the samples were lysed using RIPA (Biosharp Life Sciences) buffer (RIPA, PMSF, phosphatase inhibitor, protease inhibitor and EDTA were formulated at a ratio of 100:1:2:2:2), the protein concentration of the supernatant was determined by the BCA method. Protein samples (30 μg per lane) were separated by SDS-PAGE under reducing conditions on Novex Bis-Tris gels (4-20% acrylamide) and then transferred to PVDF membranes. The membranes were then blocked using 5% skimmed milk powder sealing solution (room temperature for 2 h) and subsequently incubated with the primary antibody overnight at 4˚C. The blots were incubated with HRP-labeled goat anti-mouse IgG (1:5,000; cat no. SA00001-1; Proteintech, Group, Inc.) at room temperature for 1 h, then developed with enhanced chemiluminescence reagents (Pierce; Thermo Fisher Scientific, Inc.) and exposed using chemiluminescence apparatus (ChemiDoc Touch; Bio-Rad Laboratories, Inc.).

Construction of a skin wound model in diabetic mice. The mice were raised in an SPF environment (temperature, 27˚C; humidity, 60-70%; noise, <60 Db; water and food were provided by the animal testing center in a standard manner). An animal model of full-thickness skin defects in diabetic mice was established to investigate the treatment effects of LIPUS combined with ADSC-Exos. Male C57BL/6 mice (4 weeks old, weighing 12-16 g) were used in this experiment. The mice were fed a high-fat diet for 2 weeks and then intraperitoneally injected with streptozotocin (STZ; Sigma-Aldrich; Merck KGaA) at a dose of 50 mg/kg. Blood samples from the caudal vein were collected from the mice every 2 days. For this, after immobilizing the mouse in a fixed box, the tail was wiped, and a blood collection needle was inserted into the tip of the tail. The tail was then pinched to drip 10 μl blood onto the test paper, and glucose levels were measured using a glucometer (Roche Diagnostics, Ltd.). Blood glucose levels >16.7 mM that lasted for >1 week were considered to indicate the successful establishment of diabetes, and these animals were eligible for subsequent experiments. A total of 55 mice were used in this study, 48 of which developed diabetes. The remaining 7 mice were euthanized by CO_2 (30% volume displacement every min). For wound generation, isoflurane was used to anesthetize mice at a concentration of 2-3% to induce anesthesia and 1.5-2% to maintain anesthesia. After shaving the hair and disinfecting the skin, a 1.0 cm diameter full-thickness wound was generated on the upper backs of the mice with surgical scissors, and a sterile alginate gel dressing was used to cover the entire wound. The humane endpoints followed in the present study included the development of any serious infections during treatment. Fortunately, no mice reached this humane endpoint and were therefore not euthanized before the end of the study.

LIPUS combined with ADSC-Exos treatment. A total of 48 mice were successfully used to construct a diabetic wound model and were randomly divided into four groups (n=12/group). All the mice in the 4 groups received one round of treatment immediately after wound establishment. Each group received the following treatments: i) The control group, subcutaneous injection of 100 μl PBS at four points (25 μl at each point) around the wound on day 0 after wound establishment; ii) the LIPUS group, treated with PBS as aforementioned in combination with LIPUS irradiation; iii) the ADSC-Exos

group, treated via subcutaneous injection of 100 μl ADSC-Exo suspension (each 100 μl injection mixture contained 70 μg ADSC-Exos) at four points (25 μl at each point) around the wound on day 0 after wound establishment; and iv) the LIPUS + ADSC-Exos group, treated with ADSC-Exo suspension as aforementioned in combination with LIPUS irradiation.

A multichannel ultrasound irradiation machine (RS232; Ultrasonic Research Institute of Chongqing Medical University, Chongqing, China) was used for LIPUS irradiation. All treatments were performed in a sterile environment. A sterile alginate gel dressing was used to cover the entire wound and the probe, and a layer of sterile coupling gel was applied between the transparent dressing on the wound surface and the transducer to ensure optimal ultrasound exposure. The transducer was fixed, and the distance between the transducer and the wound surface was maintained at ~3 mm in all experiments. The central frequency of the transducer was 1.5 MHz, and the output form was a plane and pulse wave. The mice were treated with LIPUS at an average intensity of 300 mW/cm^2, a pulse repetition rate of 1 kHz and a duty cycle of 20% for 30 min.

Wound healing evaluation. Images of the wounds were captured using a digital camera (Canon, Inc.) on days 0, 3, 7, 10 and 14 post-operation. These time points were chosen based on the procedure of wound healing, and the extent of wound healing may reflect the duration of each healing stage (30). ImageJ software (V1.8.0; National Institutes of Health) was used to measure the area of the wound. The wound healing rate was determined as follows: Wound closure rate (%)=(A0-At)/A0 x100%, where A0 represents the wound area at day 0, and At represents the wound area at days 3, 7, 10 or 14.

Histology analysis. All mice of the four groups were anesthetized using isoflurane (2-3% to induce anesthesia and 1.5-2% to maintain anesthesia) at day 14 post-operation, and wound tissues were harvested for histological analysis. The mice were then euthanized using CO_2 (injected into the box at a rate of 30% of the volume every min; the maximum flow rate did not exceed 0.5 kPa). The mice were considered dead when they maintained respiratory arrest, no motion, and pupil dilation for >5 min.

Wound samples were fixed in 4% paraformaldehyde at room temperature overnight and then dehydrated and embedded in paraffin. The samples were cut into 5-μm thick sections and mounted on slides for staining. Hematoxylin and eosin (H&E) staining (Beyotime Institute of Biotechnology) and Masson trichrome staining (Beyotime Institute of Biotechnology) were performed according to the manufacturers' instructions. The length of the scar and maturity of collagen were observed under a light microscope (BX21; Olympus Corporation).

Small animal Doppler evaluation of blood perfusion. A small animal Doppler ultrasound was used in the present study to evaluate the blood perfusion of diabetic wounds after treatment. On day 14 post-operation, the mice were anesthetized using isoflurane (2-3% to induce anesthesia and 1.5-2% to maintain anesthesia) and shaved. A laser speckle contrast imaging system (FLPI-2; Moor Instruments, Ltd.) was used to image the wounds at a constant distance and with the same dimensions to determine the area. The obtained data were then analyzed using MoorFLPI-2 Review V5.0 software (Moor Instruments, Ltd.). The mean perfusion unit (MPU) index was used to evaluate the local blood perfusion around the wounds in the different groups, and the data are presented as the ratio of the MPU of the wound area (ROI-1) to the MPU of the area surrounding the wound (ROI-2).

Immunofluorescence analysis of angiogenesis. To further evaluate angiogenesis in the wound area, immunofluorescence staining of the wound sections for CD31 (for endothelial cells; 1:1,000; cat. no. GB12063-100; Wuhan Servicebio Technology Co., Ltd.) and α-smooth muscle actin (α-SMA; 1:1,000; cat. no. GB12063-100; Wuhan Servicebio Technology Co., Ltd.), was performed on day 14. Briefly, the sections were deparaffinized and rehydrated, blocked with 5% bovine serum albumin (Beyotime Institute of Biotechnology) at room temperature for 1 h and incubated with primary antibodies overnight at 4˚C. Then, the slides were treated with Alexa Fluor 647 or Alexa Fluor 488 secondary antibodies (1:5,000; cat. nos. ab150115 and ab150117; Abcam) at room temperature for 2 h, and the nuclei were stained with 4,6-diamidino-2-phenylindole (DAPI; Beyotime Institute of Biotechnology) at room temperature and observed immediately. All slides were then observed under a fluorescent microscope (BX21; Olympus Corporation), and the number of newly formed and mature vessels was calculated in five random fields per section between wound edges using ImageJ software.

ADSC-Exos uptake in vivo. To evaluate the effect of LIPUS irradiation on ADSC-Exos metabolism, full-thickness wounds on 10 diabetic mice (in addition to the 48 mice described above) were generated as aforementioned. ADSC-Exos were labeled using DiR (Shanghai Yuanye Biotechnology Co., Ltd.) and subcutaneously injected at four points around the wound as aforementioned. In total, 5 mice were irradiated immediately after injection and the remaining 5 mice were covered with sterile dressings and returned to the cage. The distribution of exosome fluorescence *in vivo* was observed using a small animal imaging system (PerkinElmer, Inc.) at 1, 2, 6, 24 and 36 h after injection. The fluorescence signal intensity was analyzed using Living Image software (version 4.4; PerkinElmer, Inc.).

To further evaluate the uptake of exosomes in the targeted area, an additional 10 diabetic mice were treated as aforementioned, except using DiI-labeled ADSC-Exos. The wound and surrounding skin tissues were harvested for frozen section preparation and examination 48 h after DiI-labeled ADSC-Exos subcutaneous injection and LIPUS treatment, following euthanasia as aforementioned. After the preparation of frozen sections (8-μm) in liquid nitrogen, the nuclei were stained with DAPI at room temperature, and fluorescence was observed immediately by laser scanning confocal microscopy (FV1200; Olympus Corporation). ImageJ software was used for analysis.

ADSC-Exos uptake in vitro. To further verify whether LIPUS can promote exosome uptake *in vitro*, immortalized human umbilical vein endothelial cells (HUVECs; cat. no. CL-191 h; Wuhan Saios Biotechnology Co., Ltd.) were divided into the

four following groups: The control, LIPUS, ADSC-Exos and LIPUS + ADSC-Exos groups. The LIPUS and ADSC-Exo groups were treated with LIPUS or ADSC-Exos alone. The LIPUS + ADSC-Exos group was treated with 10 μl exosomes (100 μg/ml) combined with LIPUS irradiation. The aforementioned multichannel ultrasound irradiation machine was used for LIPUS irradiation. The ultrasonic transducer was placed under the cell culture plate and a coupling agent was used to ensure the probe fully contacted the plate. The central frequency of the transducer was 1.5 MHz, and the output form was a plane wave and pulse wave. HUVECs were treated with LIPUS at an average intensity of 30 mW/cm^2, a pulse repetition rate of 1 kHz and a duty cycle of 20% for 30 min.

The ADSC-Exos were labeled using a DiI fluorescent labeling kit (Invitrogen; Thermo Fisher Scientific, Inc.). Briefly, ADSC-Exos were incubated with 5 μM DiI dye at 37˚C for 15 min in the dark and then centrifuged at 12,000 x g for 15 min to remove free DiI dye. The supernatant was removed, and the labeled ADSC-Exos were resuspended in PBS before use. Subsequently, the HUVECs were incubated with DiI-labeled ADSC-Exos at a dose of 5 μg/ml for 6 h. After removing the supernatant and washing with PBS, the samples were fixed with 4% paraformaldehyde at room temperature for 15 min and washed with PBS three times. The fixed samples were stained with 10 μg/ml DAPI (Invitrogen; Thermo Fisher Scientific, Inc.) at room temperature. After washing with PBS three times, the uptake of ADSC-Exos by HUVECs was observed using a fluorescent microscope (Olympus Corporation). The DiI fluorescence intensity in the HUVECs was quantified using ImageJ software.

Angiogenesis in vitro. To investigate the effect of LIPUS on angiogenesis after the cellular uptake of ADSC-Exos, Cell Counting Kit-8 (CCK-8), scratch wound healing and tube formation assays were conducted.

The CCK-8 (Dojindo Laboratories, Inc.) assay was conducted to analyze cell viability, following the manufacturer's protocol. HUVECs were seeded into 96-well plates (5x10^3 cells/well in 100 μl culture medium) and treated as aforementioned. After incubation of the HUVECs at 37˚C for 24 h, 10 μl of CCK-8 was added to each well. After a further incubation at 37˚C for 4 h, the absorbance was measured at 450 nm using an automatic microplate reader (PerkinElmer, Inc.). All experiments were repeated three times.

A scratch wound healing assay was conducted to assess the migration capability of HUVECs. Briefly, 5x10^5 HUVECs were seeded into a 6-well cell culture plate with culture medium supplemented with 10% FBS. When the cell confluency reached 90%, the cell monolayer was scraped in a straight line with a 200-μl pipette tip. The cells were treated as aforementioned and cultured for 24 h in FBS-free medium. Images of five fields of view were collected at 0 and 24 h using an inverted microscope (Olympus Corporation), and the decrease in the wound area was quantified using ImageJ software.

A tube formation assay was conducted to assess the proangiogenic effects of the different treatments. HUVECs (5x10^5 cells) were seeded into Matrigel-coated 6-well cell culture plates with FBS-free medium and treated as aforementioned. After incubation for 4 h in 5% CO_2 at 37˚C, the total number of branching points and the total tube length of the cells were observed using an inverted microscope (Olympus Corporation). ImageJ software was used to analyze the images and count the tubes.

Statistical analysis. All experiments were performed in triplicate. The data are presented as the mean ± standard deviation. Differences between two groups were analyzed by unpaired Student's t-tests and differences between multiple groups were analyzed by one-way ANOVA, followed by Tukey's post hoc test for pairwise comparisons. Statistical analysis was conducted using SPSS software (version 26; IBM Corp.). $P<0.05$ was considered to indicate a statistically significant difference.

Results

Characterization of ADSC-Exos. The third-passage ADSCs exhibited a spindle-like morphology, as observed under a light microscope (Fig. 2A). The osteogenic and adipogenic differentiation ability of the ADSCs (assessed using osteogenic and adipogenic differentiation medium kits) confirmed the multilineage differentiation potential of the cell line (Fig. 2B and C). The flow cytometry analysis of surface marker expression is shown in Fig. 2D. The ADSCs were positive for the mesenchymal stem cell (MSC) markers, CD29 (99.87%) and CD90 (99.76%), but negative for the hematopoietic stem cell marker, CD34 (2.94%).

ADSC-Exos were identified by TEM and western blotting analysis. According to the TEM images, the ADSC-Exos exhibited a spherical or cup-shaped structure (Fig. 2E). Particle size measurements indicated that the median size of the ADSC-Exos was 133 nm (Fig. 2F). Western blotting analysis demonstrated that the ADSC-Exos were positive for the specific exosome surface markers, CD9 and Tsg 101 (Fig. 2G). Collectively, these results indicated that ADSC-Exos had been successfully harvested.

LIPUS combined with ADSC-Exos treatment accelerates diabetic wound healing. Representative gross observation images of the diabetic wound healing process at different time points are displayed in Fig. 3A. From day 10, the mice developed black hairs around the wound area, which could not be removed, so the skin appeared dark blue. The wounds treated with LIPUS + ADSC-Exos healed faster than those in the other groups throughout the entire healing duration. LIPUS, as well as ADSC-Exo, only treatment also demonstrated faster healing compared with the diabetic control. On the third day after treatment, the wound area in the LIPUS + ADSC-Exos group was significantly reduced, while those in the control and LIPUS groups were only slightly changed ($P<0.05$; Fig. 3B). At day 10, only the LIPUS + ADSC-Exo-treated animals achieved complete wound closure (wound closure rate >95%). On day 14, the wounds in all groups except the control group were covered with neo-epidermis. However, the wound surface of the LIPUS + ADSC-Exo-treated animals was the flattest. Further quantitative analysis also confirmed that the wound healing rates at days 3, 7, 10 and 14 were significantly higher in the LIPUS + ADSC-Exos group compared with the control group, followed by the rates in the ADSC-Exos group and the LIPUS group (Fig. 3B).

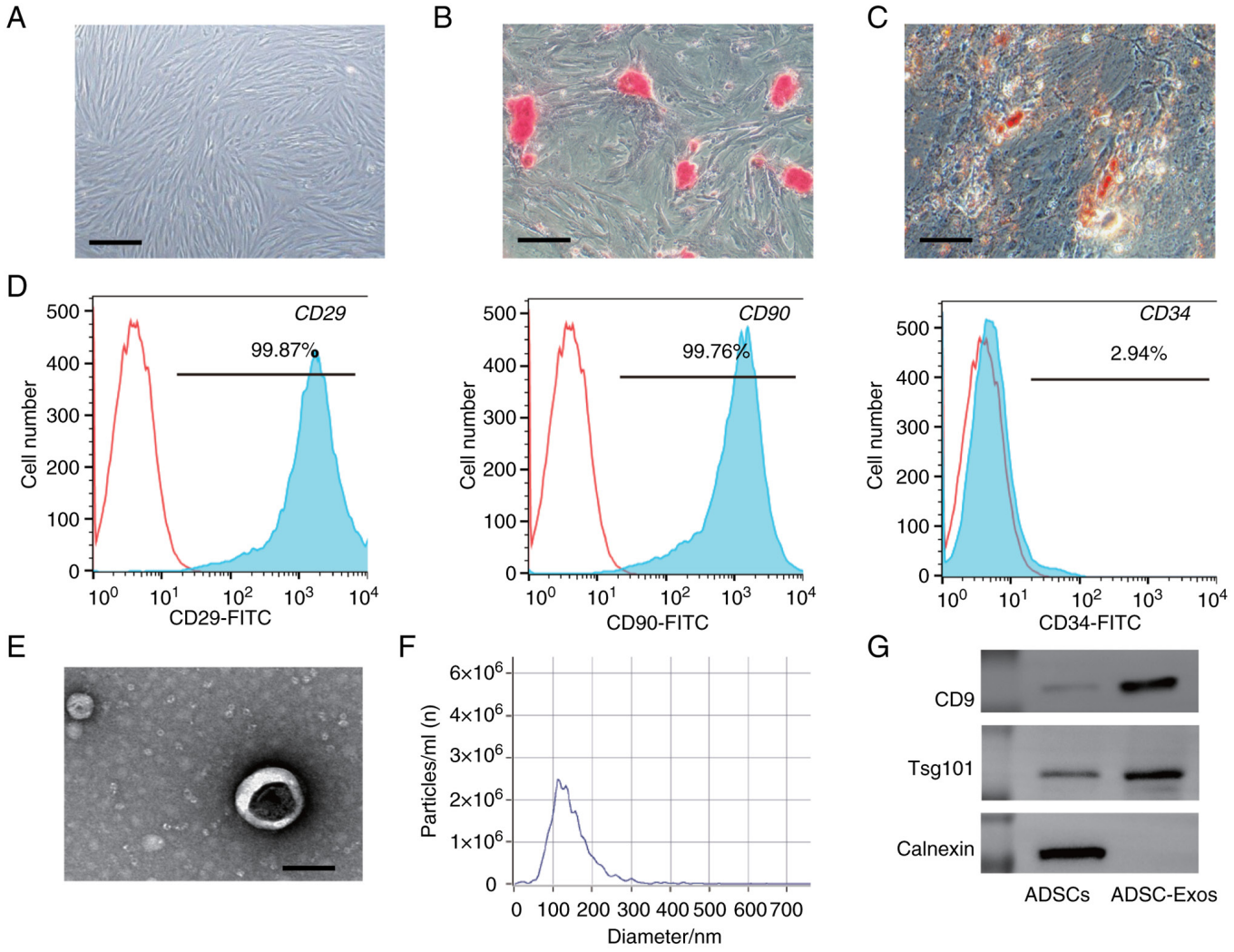

Figure 2. Characterization of ADSC-Exos. (A) Representative images of third-generation ADSCs. Scale bar, 200 μm. Representative images of (B) adipogenesis and (C) osteogenesis of ADSCs stained with oil red O (scale bar, 50 μm) and alkaline phosphatase (scale bar, 100 μm), respectively. (D) Flow cytometry analysis of ADSC surface marker expression. (E) Representative image of ADSC-Exo morphology by transmission electron microscopy. Scale bar, 100 nm. (F) Size distribution of ADSC-Exos. (G) Western blotting analysis of CD9 and Tsg 101 expression in ADSC-Exos. ADSC, adipose-derived stem cell; ADSC-Exos, exosomes derived from ADSCs; Tsg101, tumor susceptibility gene 101.

The results of H&E staining of the wound samples demonstrated that the thickness, differentiation status of the neo-epidermis and length of the wound area in the LIPUS + ADSC-Exos group were significantly shorter than those in the control and ADSC-Exo groups at day 14 (Fig. 4A and B).

Masson's staining was used to reveal collagen deposition and remodeling in the diabetic wounds following different treatments (Fig. 4C). The amount of collagen in all three treatment groups was notably greater than in the control group at day 14, and the amount of collagen fiber was the highest in the LIPUS + ADSC-Exos group. Moreover, the collagen fibers in the LIPUS + ADSC-Exos group had more organized structures with higher fiber density and greater blood vessel formation compared with the LIPUS and ADSC-Exos groups. Collectively, these results suggested that LIPUS + ADSC-Exos accelerated collagen deposition and remodeling in the diabetic wound healing process.

LIPUS combined with ADSC-exos treatment increases angiogenesis in diabetic wounds. CD31 and α-SMA immunofluorescence staining was performed to evaluate the newly formed and relatively mature blood vessels on day 14. Mature blood vessels provide a continuous and stable supply of blood to tissues and are composed of vascular endothelial cells and smooth muscle cells. Therefore, the staining of vascular endothelial cells (against CD31) and smooth muscle cells (against α-SMA) was used to judge the number of mature vessels in the present study. As shown in Fig. 5A, little positive staining was observed in the control group. The LIPUS + ADSC-Exos group exhibited the highest expression of CD31 and α-SMA, followed by the ADSC-Exo-treated group, while the LIPUS treatment group showed a low level of positive staining. The number of vessels connected to the smooth muscle cells were also counted, according to the α-SMA staining results (Fig. 5B). The number of mature vessels in the LIPUS + ADSC-Exos group was 35.12±1.93 per field, which was higher than the numbers observed in the other three groups. The numbers of mature vessels in the ADSC-Exos and LIPUS treatment groups were 20.25±1.44 and 9.41±0.98 per field, respectively. These results indicated that LIPUS +

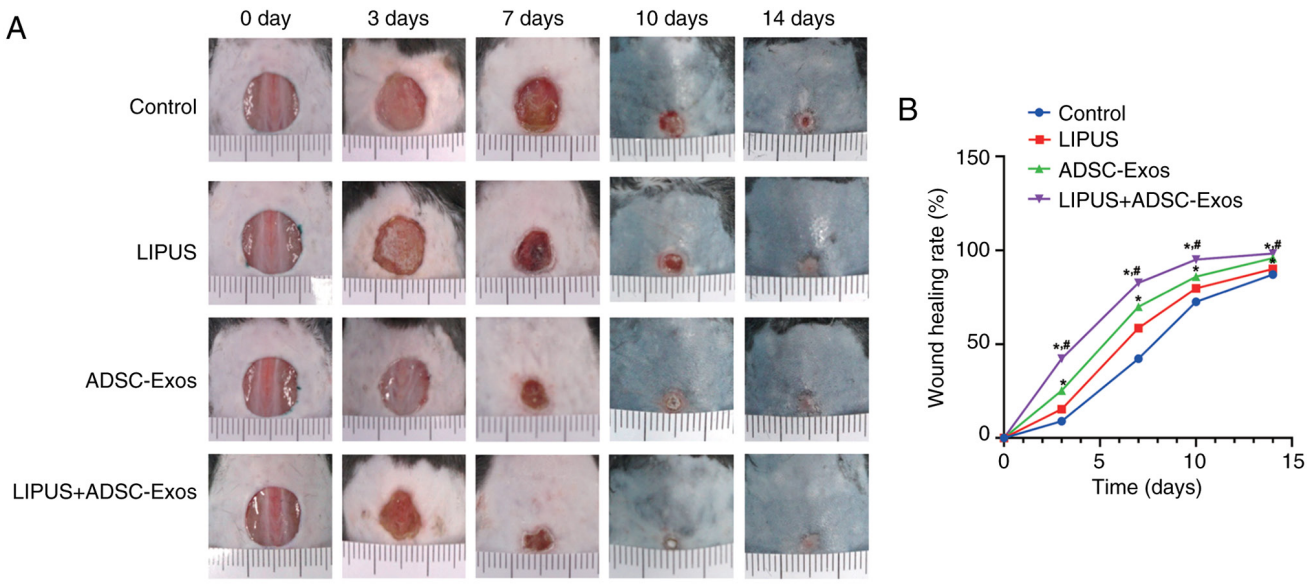

Figure 3. The healing process of diabetic wounds *in vivo*. (A) Representative images of diabetic wound healing in mice treated with PBS (control), LIPUS, ADSC-Exos or LIPUS + ADSC-Exos 0, 3, 7, 10 and 14days post-operation. Scale bar, 1 mm per graduation. (B) Wound healing closure rates were calculated among the different groups using ImageJ software. *P<0.05 vs. control group; $^{\#}$P<0.05 vs. ADSC-Exos group. ADSC-Exos, exosomes derived from adipose-derived stem cells; LIPUS, low-intensity pulsed ultrasound.

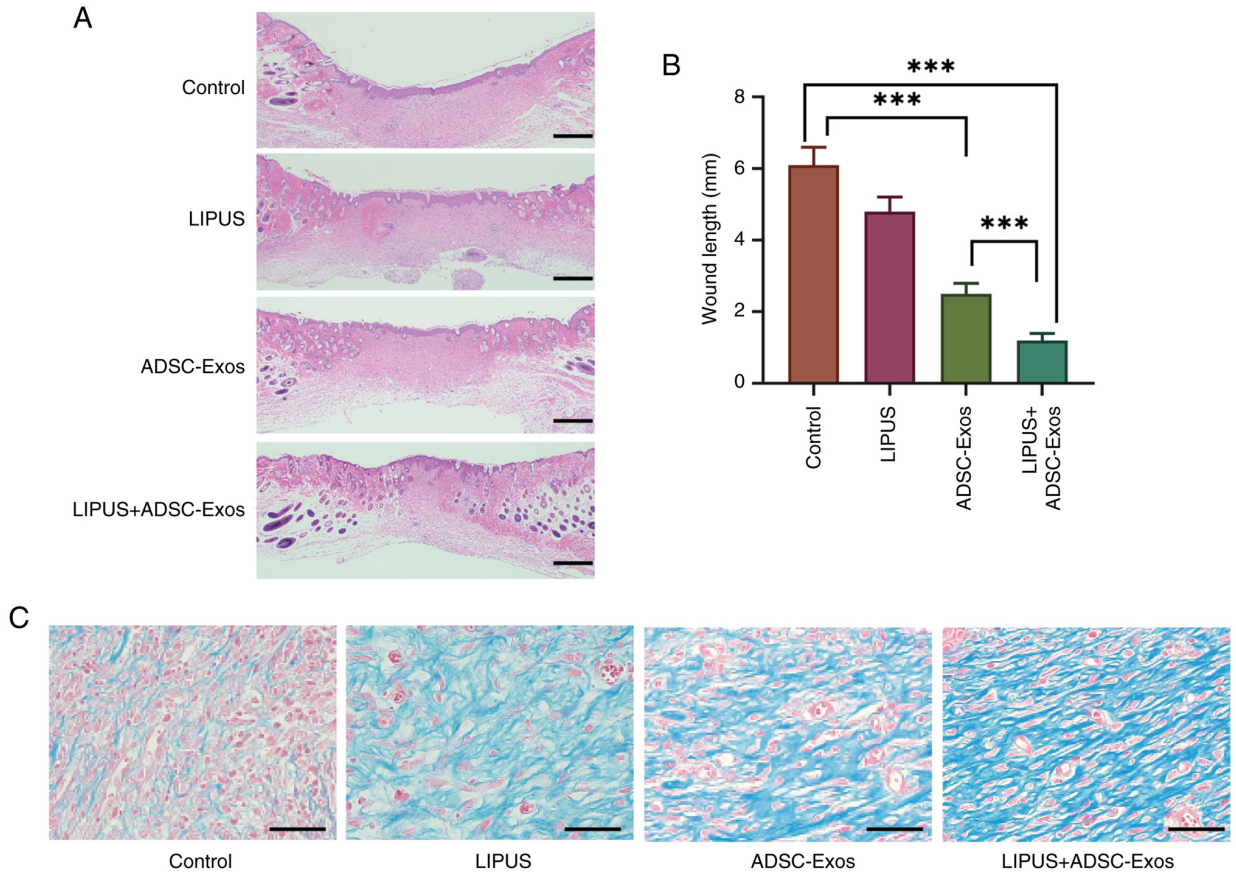

Figure 4. Histological analysis of diabetic wounds. (A) Representative hematoxylin and eosin-stained images of wounds on day 14 following different treatments. Scale bar, 200 μm. (B) Quantification of the length of the wound area on day 14. ***P<0.001. (C) Representative Masson's-stained images showing collagen deposition in the wound area. Scale bar, 50 μm. ADSC-Exos, exosomes derived from adipose-derived stem cells; LIPUS, low-intensity pulsed ultrasound.

ADSC-Exos treatment efficiently promoted angiogenesis in diabetic wounds.

LIPUS combined with ADSC-Exos treatment enhances blood perfusion of diabetic wounds. Small animal Doppler

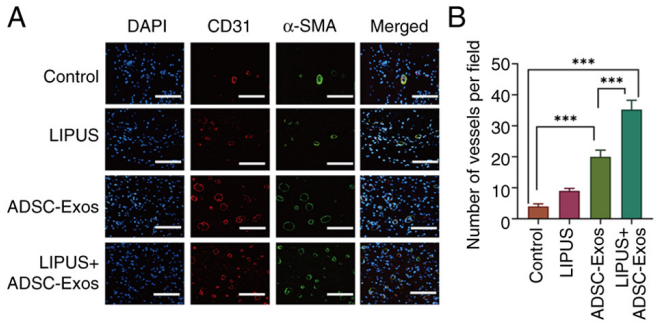

Figure 5. Assessment of angiogenesis in diabetic wounds. (A) Representative images of immunofluorescence staining for CD31 and α-SMA, indicating newly formed and mature vessels. Scale bar, 200 μm. (B) Quantification of the number of mature blood vessels in the wound beds on day 14. ***P<0.001. α-SMA, α-smooth muscle actin; ADSC-Exos, exosomes derived from adipose-derived stem cells; DAPI, 4,6-diamidino-2-phenylindole; LIPUS, low-intensity pulsed ultrasound.

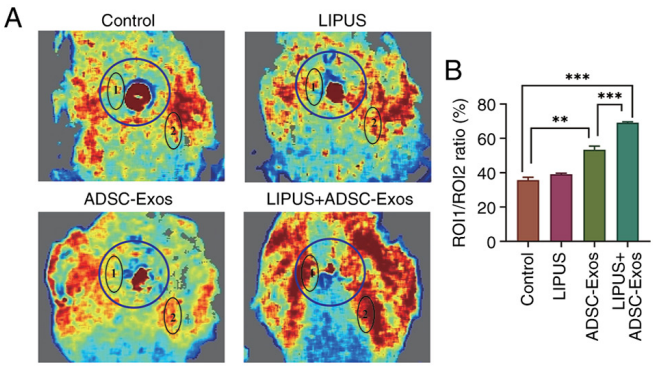

Figure 6. Blood perfusion imaging *in vivo*. (A) Blood perfusion of the wound was assessed using a small animal Doppler ultrasound. (B) Quantitative comparison of different treatment groups. Blood perfusion is presented as the ROI-1/ROI-2 ratio to avoid individual differences between mice. **P<0.01, ***P<0.001. ROI-1, ratio of wound area; ROI-2, normal area surrounding the wound. ADSC-Exos, exosomes derived from adipose-derived stem cells; LIPUS, low-intensity pulsed ultrasound.

ultrasound was used in the present study to non-invasively monitor blood perfusion of skin wounds and the surrounding areas before the mice were sacrificed. At 14 days after treatment, laser specular blood flow imaging indicated that the ROI-1/ROI-2 ratios of the control, LIPUS, ADSC-Exos and LIPUS + ADSC-Exos groups were 35.76±1.63, 39.09±0.58, 53.39±2.07 and 69.13±0.53%, respectively (P<0.05; Fig. 6). All three treatments improved blood perfusion in the wound and surrounding area, but the animals treated with LIPUS + ADSC-Exos demonstrated the most improvement. Compared with the control, LIPUS, ADSC-Exos and LIPUS + ADSC-Exos increased the ROI-1/ROI-2 ratio by 3.33, 17.63 and 33.37%, respectively. These results suggested that LIPUS + ADSC-Exos significantly improved blood perfusion around the wound, and the effect was greater than the sum of the LIPUS and ADSC-Exos treatments alone.

LIPUS promotes uptake of ADSC-Exos in vivo. To explore whether the effective angiogenesis therapy of LIPUS + ADSC-Exos was achieved by LIPUS promoting ADSC-Exo uptake, the distribution and duration of DiR-labeled ADSC-Exos around the wound were observed via *in vivo* imaging. At 2, 6, 24 and 36 h after treatment, the exosome fluorescence in the LIPUS irradiation group was more widely distributed, completely covered the wound, was stronger and lasted longer (Fig. 7). In the group treated with ADSC-Exos alone, fluorescence was mainly limited to the four injection sites. At 36 h, strong fluorescence could still be observed throughout the wound in the mice that received LIPUS irradiation, while only weak spotted fluorescence was observed in the group without LIPUS irradiation. Quantitative analysis showed that the exosome fluorescence intensity in the LIPUS irradiation group was 1.50, 4.05, 2.81, 4.51 and 5.33-fold higher compared with the without LIPUS irradiation group at 1, 2, 6, 24 and 36 h, respectively (Fig. 7B). These results indicated that LIPUS irradiation improved the distribution of ADSC-Exos, promoted the uptake of exosomes in the injured area and prolonged the action time of exosomes.

Confocal microscopy demonstrated that the percentage of cells with visible DiI fluorescence around the wound was 41.20±1.11% after LIPUS irradiation, which was higher than

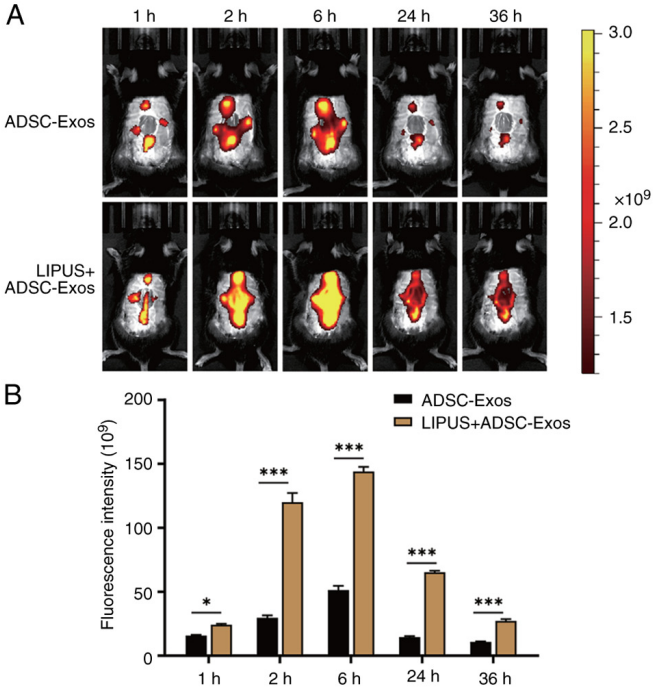

Figure 7. *In vivo* imaging of ADSC-Exos. (A) Small animal *in vivo* imaging demonstrated the distribution of DiR-labeled ADSC-Exos. (B) Quantitative comparison of the fluorescence intensity at different time points. *P<0.05, ***P<0.001. ADSC-Exos, exosomes derived from adipose-derived stem cells; LIPUS, low-intensity pulsed ultrasound.

the non-irradiated group (23.16±1.16%) (Fig. 8). These results confirmed that LIPUS promoted the uptake of exosomes in the wound area, which may be why LIPUS + ADSC-Exos treatment promoted angiogenesis and accelerated diabetic wound repair.

LIPUS promotes cellular uptake of ADSC-Exos in vitro. To verify that LIPUS + ADSC-Exo therapy promoted angiogenesis by promoting exosome uptake *in vitro*, ADSC-Exos were labelled with DiI. The efficiency of exosome uptake in the different treatment groups was then compared by measuring

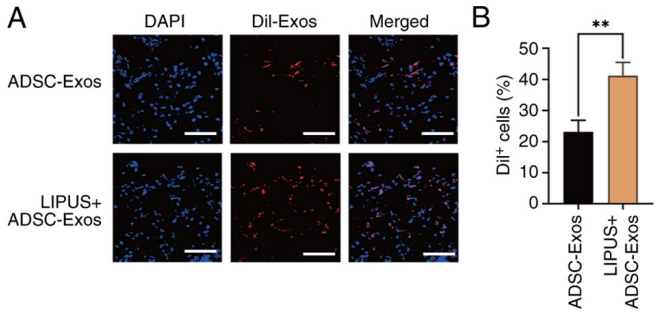

Figure 8. Uptake of ADSC-Exos *in vivo*. (A) Distribution of DiI-labeled ADSC-Exos in skin tissue. Scale bar, 200 μm. (B) Quantitative comparison of the percentage of DiI$^+$ cells, **P<0.01. ADSC-Exos, exosomes derived from adipose-derived stem cells; DAPI, 4,6-diamidino-2-phenylindole; LIPUS, low-intensity pulsed ultrasound.

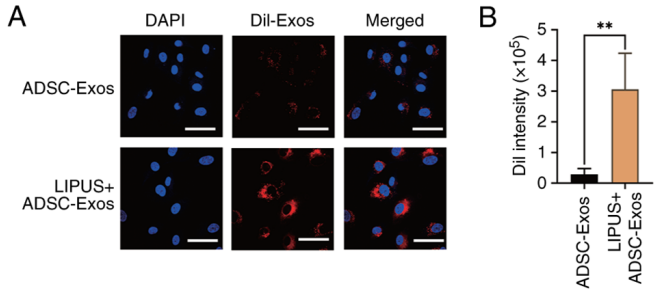

Figure 9. Cellular uptake of ADSC-Exos. (A) Representative fluorescence images of HUVEC uptake of ADSC-Exos with or without LIPUS irradiation. Scale bar, 50 μm. (B) Quantitative analysis of the DiI intensity. **P<0.01. ADSC-Exos, exosomes derived from adipose-derived stem cells; DAPI, 4,6-diamidino-2-phenylindole; HUVECs, human umbilical vein endothelial cells; LIPUS, low-intensity pulsed ultrasound.

the fluorescence intensity in the HUVECs. Representative confocal microscopy images shown in Fig. 9A demonstrated that the nuclei of HUVECs were labeled in blue (DAPI) and that the red fluorescence of DiI-labeled ADSC-Exos was clearly observed in the cytoplasm. Quantitative analysis shown in Fig. 9B demonstrated that the DiI fluorescence intensity of HUVECs in the LIPUS + ADSC-Exos group was 10.93-fold higher than the ADSC-Exos group, suggesting that LIPUS significantly increased the uptake of exosomes by HUVECs.

LIPUS enhances angiogenesis by promoting the cellular uptake of ADSC-Exos in vitro. The angiogenic effects of HUVECs were evaluated through CCK-8, scratch wound healing and tube formation assays. The CCK-8 assay demonstrated that the OD value in the LIPUS + ADSC-Exos group was 1.88±0.14, which was higher than that of the ADSC-Exos (0.65±0.03), LIPUS (0.63±0.03) and control (0.46±0.04) groups (Fig. 10C). The CCK-8 results therefore indicated that HUVECs treated with LIPUS + ADSC-Exos exhibited a much higher viability than HUVECs in the other treatment groups. The scratch wound healing assay demonstrated that the LIPUS + ADSC-Exos group had the smallest gap following wound closure and therefore the greatest cell migration ability (Fig. 10A and D). The results of the tube formation assay indicated that the LIPUS + ADSC-Exos group exhibited better tube formation (characterized by a greater total tube length and complete tubular structure) than the other three groups (Fig. 10B and E). Compared with the LIPUS and ADSC-Exos groups, the LIPUS + ADSC-Exos treatment group formed more lumens, had larger lumen circumferences and more mature structures. Collectively, these results confirmed that LIPUS + ADSC-Exos treatment effectively promoted angiogenesis *in vitro*.

Discussion

In the present study, the therapeutic effects of LIPUS on ADSC-Exo-mediated diabetic wound healing were investigated. The results demonstrated that treatment with ADSC-Exos alone moderately contributed to diabetic wound healing, but the combination of ADSC-Exos and LIPUS significantly promoted angiogenesis and accelerated cutaneous wound healing. *In vivo* imaging demonstrated that LIPUS promoted the uptake of ADSC-Exos in the wound area and improved the utilization efficiency of exosomes. The *in vitro* results further confirmed that LIPUS enhanced the uptake efficiency of ADSC-Exos by 10.93-fold and significantly increased the proliferation, migration and tubular formation abilities of HUVECs. Therefore, the present study, to the best of our knowledge, illustrated for the first time that LIPUS can improve ADSC-Exo-mediated diabetic wound healing by promoting cellular uptake of exosomes and enhancing angiogenesis.

Diabetic wounds are one of the most common and serious complications of diabetes mellitus. Impaired angiogenesis is an important reason for the prolonged wound healing time in diabetic patients (31). A number of methods, including different types of dressings, tissue-engineered skin substitutes, growth factors and hyperbaric oxygen, have been used in the treatment of non-healing diabetic wounds. However, the results have not been completely satisfactory. Accumulating evidence has suggested that stem cell-derived exosomes have great potential in promoting diabetic wound healing through the induction of therapeutic angiogenesis. Hu *et al* (32) demonstrated that exosomes derived from bone MSCs (BMSCs) that were pretreated with pioglitazone accelerated diabetic wound healing by promoting angiogenesis through PI3K/AKT/endothelial nitric oxide synthase pathway activation. In addition, Yan *et al* (33) found that human umbilical cord MSC-derived exosomes accelerated diabetic wound healing by ameliorating oxidative stress and promoting angiogenesis. Although various stem cell-derived exosomes potentially exert therapeutic effects on diabetic wound healing, their biological properties are different. A comparative study demonstrated that BMSC-derived exosomes mainly promoted proliferation, whereas ADSC-derived exosomes had a major effect on angiogenesis (34). Therefore, ADSC-Exos were chosen as the therapeutic agent for angiogenesis in the present study.

Although ADSC-Exos are safe, effective and convenient to use, their low yield and short half-life make it difficult to meet the requirements of clinical treatment. As the exosome yield cannot be significantly increased, improving its utilization efficiency is the only feasible approach. Previous studies have shown that LIPUS, which acts as a low-intensity mechanical stimulus, can increase cell deformation and membrane permeability, promote metabolite exchange, regulate cell function

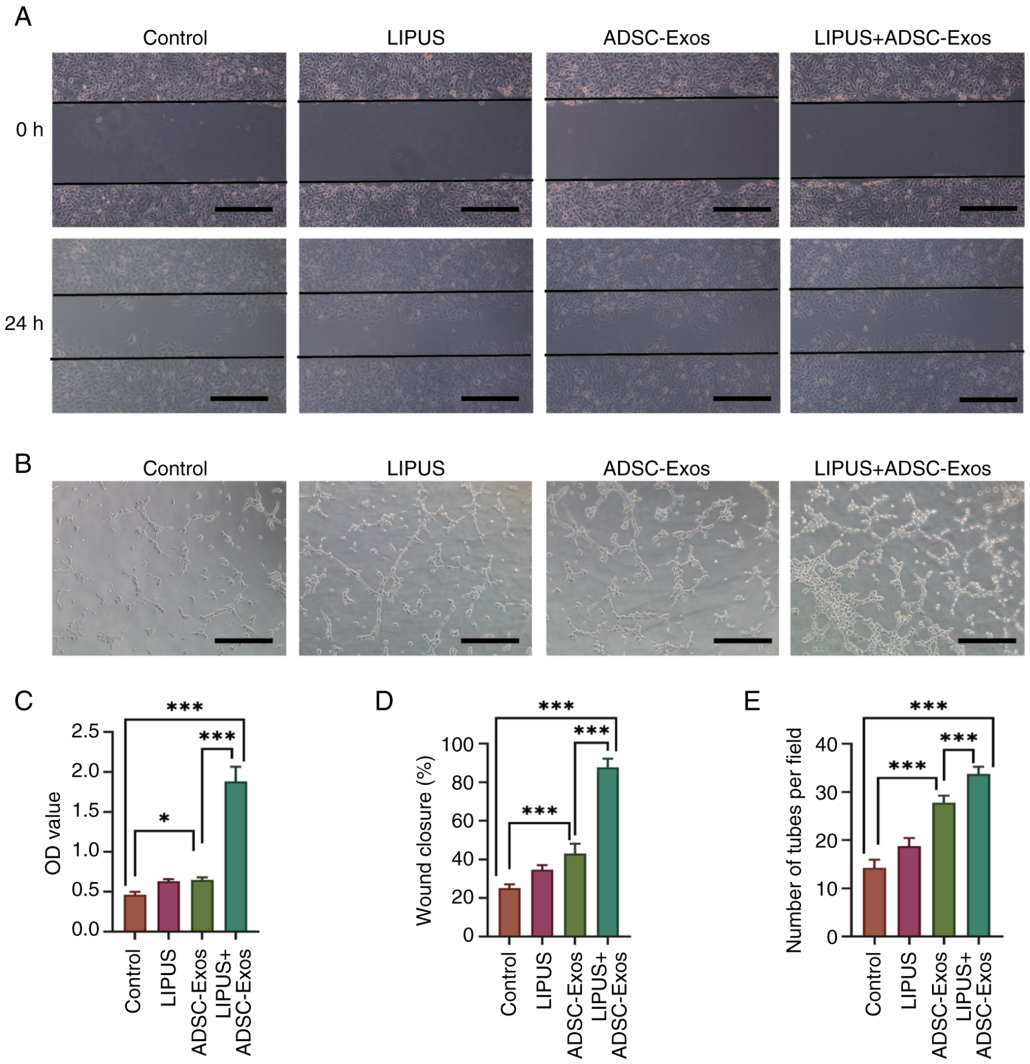

Figure 10. Angiogenic effects of treatment *in vitro*. (A) A scratch wound healing assay was used to assess the cell migration of HUVECs following treatment. Scale bar, 200 μm. (B) A tube formation assay was performed to visualize the cell capillary network formation of HUVECs following treatment. Scale bar, 100 μm. (C) The CCK8 assay was conducted to assess HUVEC viability. (D) Quantitative analysis of cell migration (wound healing assay) in the four groups. (E) Quantitative analysis of tube formation in the four groups. *P<0.05, ***P<0.001. ADSC-Exos, exosomes derived from adipose-derived stem cells; HUVECs, human umbilical vein endothelial cells; LIPUS, low-intensity pulsed ultrasound.

and exert a variety of biological effects (35-37). However, whether LIPUS can enhance the utilization efficiency of exosomes remains unknown.

The results of the present study demonstrated that LIPUS combined with ADSC-Exos treatment significantly promoted the repair of diabetic wounds. Compared with ADSC-Exos alone, the average wound healing time in the combined treatment group was 4 days shorter, and the new skin was more mature and complete. Immunofluorescence and small animal Doppler ultrasound indicated that the combined therapy significantly increased angiogenesis and blood perfusion in the wound area. These results suggested that the combined therapy accelerated the healing of diabetic wounds mainly by promoting angiogenesis. However, whether the effective angiogenesis of LIPUS + ADSC-Exos therapy is achieved by LIPUS promoting ADSC-Exos uptake still needs to be explored further.

In the present study, to observe the metabolism of exosomes *in vivo*, ADSC-Exos were labeled with DiR. *In vivo* imaging demonstrated that LIPUS promoted the distribution of ADSC-Exos in the wound area, increased the fluorescence intensity of target tissue and prolonged the duration of the exosomes. Quantitative analysis showed that the fluorescence intensity of DiR-labeled ADSC-Exos in the LIPUS irradiation group was 5.33-fold higher than in the non-irradiation group 36 h after treatment. This result indicated that LIPUS effectively increased the uptake of exosomes and reduced metabolic clearance, thus improving the utilization efficiency of exosomes *in vivo*. In summary, these results suggested that LIPUS irradiation may improve the uptake of ADSC-Exos, thus enhancing therapeutic angiogenesis and accelerating the repair of diabetic wounds.

Immortalized HUVECs cell line is widely used as the cell model in vascular endothelial cell experiments. Immortalized HUVECs are the closest to original human endothelial cells and have the ability to form tubes, which is the basic characteristic of endothelial vascularization. In addition, HUVECs have stem cell potential and remain stable for 50 generations (38). While aortic and coronary endothelial cell lines are more consistent with the characteristics of cardiovascular endothelial cells, they are mainly used in the study of atherosclerosis

and are not suitable for simulating the peripheral microvascular conditions caused by diabetes. In the present study, to further verify the underlying mechanism by which LIPUS promotes the cellular uptake of exosomes and enhances angiogenesis *in vitro*, ADSC-Exos were labeled with the fluorescent dye, DiI, and the uptake of exosomes by immortalized HUVECs was observed. The results demonstrated that LIPUS significantly increased the cellular uptake of exosomes by 10.8-fold *in vitro* and that DiI-labeled ADSC-Exos were mainly localized in the cytoplasm. Furthermore, compared with ADSC-Exo treatment alone, the combination of ADSC-Exos with LIPUS irradiation significantly increased the proliferation, migration and tube formation abilities of HUVECs *in vitro*. These results confirmed that LIPUS promoted the uptake of ADSC-Exos and improved the utilization efficiency of exosomes, thus enhancing therapeutic angiogenesis.

Certain mechanisms have been proposed that may explain why LIPUS increased the cellular uptake of ADSC-Exos *in vivo* and *in vitro*. For example, LIPUS irradiation produces a stable cavitation effect in the target area, which causes microbubbles (as the gas nucleus in the liquid environment) to continuously expand and shrink, thus forming a microstream (39). The microstream can cause exosomes to spread in different directions and therefore expand the distribution of exosomes in the wound area. In the present study, fluorescently labeled ADSC-Exos were subcutaneously injected at four points around the wound area and, 2 h after LIPUS irradiation, ADSC-Exos diffused in different directions and covered the entire wound area. In the group treated with ADSC-Exos alone, fluorescence was mainly limited to the four injection sites. In addition, a stable cavitation effect can promote contact between exosomes and target cells and increase the permeability of cell membranes, thus significantly improving the endocytosis of target cells (40). Rapid diffusion and endocytosis significantly increase exosome uptake and reduce immune clearance, thus improving exosome utilization efficiency. In the present study, *in vivo* imaging demonstrated that 36 h after LIPUS irradiation, a large amount of fluorescence covering the wound was still observed in the combined treatment group, while only weak dot-like fluorescence was observed in the group treated with exosomes alone. This result confirmed that LIPUS reduced the immune clearance of exosomes and prolonged the duration of exosome treatment.

LIPUS, a non-invasive localized mechanical stimulus, exerts a variety of therapeutic biophysical effects and has been used to treat a number of diseases such as ligament trauma, fracture, arthromeningitis and neurodegenerative disorders (41). The use of LIPUS for improving bone regeneration has been approved by the US Food and Drug Administration for human application. However, the molecular mechanisms of the therapeutic effects of LIPUS remain unclear. A study has suggested that LIPUS 'massages' cells and can activate multiple signaling pathways through energy transmission (42). Razavi *et al* (43) found that LIPUS downregulated pro-inflammatory cytokines (IL-1β, IL-2, IL-6, IFN-γ, IFN-γ-induced protein 10 and TNF-α), and Burks *et al* (44) suggested that LIPUS exposure induced the upregulation of some signaling [such as VEGF, fibroblast growth factor (GF), placental GF, hepatocyte GF and stromal derived factor-1α] and cell adhesion (such as intercellular adhesion molecule 1 and vascular cell adhesion molecule 1) molecules on muscle vasculature. Yoon *et al* (45) have suggested that pulsed focused ultrasound can mediate MSC homing by mechanically opening transient receptor potential cation channel subfamily C member 1 on the plasma membrane, causing an influx of sodium and calcium that depolarizes the membrane and activates the voltage-gated calcium channel, causing further calcium influx and activating NF-κB and cyclooxygenase-2. These studies suggest that LIPUS may promote wound healing by inhibiting the inflammatory pathway and enhancing the regeneration of tissue. Since LIPUS can activate cellular signaling pathways and since exosomes are important molecules in intercellular communication, we hypothesize that the combination of LIPUS and exosomes might exert synergistic effects that enhance intercellular communication. However, this hypothesis requires further exploration.

Although the results of the present study revealed that LIPUS significantly improved the therapeutic effect of ADSC-Exos in diabetic wound repair by enhancing the cellular uptake of exosomes, there were also some limitations to the study. First, the etiology and pathophysiological processes of diabetes are complex, and it is difficult to construct an animal model that conforms to the pathophysiology of human diabetes. Spontaneous models of diabetes such as NOD mice, and single-gene obesity models such as $Lep^{ob/ob}$ mice, are commonly used in research, but these particular strains may not develop the corresponding complications and are very expensive (46). In the present study, intraperitoneal injection of STZ after a period of high-fat feeding had a high success rate of diabetes induction in mice and could be used to evaluate drug efficacy. However, this model still may not represent the true condition of patients with diabetes. Second, in addition to improving the efficiency of ADSC-Exos uptake, LIPUS is likely to exert synergistic effects with ADSC-Exos. The mechanisms underlying these synergistic effects may be complicated and further studies are needed to elucidate them.

In conclusion, the present study explored a novel method to enhance the therapeutic effects of ADSC-Exos in diabetic wound healing by combining administration with LIPUS. The results demonstrated that LIPUS significantly improved the uptake of exosomes *in vivo* and *in vitro*, thus improving the utilization efficiency of ADSC-Exos and enhancing angiogenesis. As a non-invasive and convenient technology, LIPUS may provide a promising strategy for enhancing exosome-mediated diabetic wound repair.

Acknowledgements

Not applicable.

Funding

This study was supported by The National Natural Science Foundation of China (grant nos. 81901759, 81971624, 81901757 and 82102045).

Availability of data and materials

The datasets used and/or analyzed during the current study are available from the corresponding author on reasonable request.

Authors' contributions

QZ and SC made contributions to the conception of the study. QD initiated and designed the research. FZ and JL performed the experiments and acquired the raw data. LY, BG, HW and NJ contributed to data analysis and interpretation. QD and FZ wrote the first draft of the manuscript, and SC and QZ critiqued and modified the manuscript. QD and FZ confirm the authenticity of all the raw data. All authors have read and approved the final version of the manuscript.

Ethics approval and consent to participate

All animal experiments were conducted in accordance with the National Institutes of Health Guide for the Care and Use of Laboratory Animals (NIH Publications No. 8023, revised 1978). The animal protocols were approved by The Laboratory Animal Care and Use Committee of Renmin Hospital, Wuhan University (Wuhan, China; approval nos. 20210210 and 20210506).

Patient consent for publication

Not applicable.

Competing interests

All authors declare that they have no competing interests.

References

1. Saeedi P, Petersohn I, Salpea P, Malanda B, Karuranga S, Unwin N, Colagiuri S, Guariguata L, Motala AA, Ogurtsova K, *et al*: Global and regional diabetes prevalence estimates for 2019 and projections for 2030 and 2045: Results from the International Diabetes Federation Diabetes Atlas, 9th edition. Diabetes Res Clin Pract 157: 107843, 2019.
2. International Working Group on the Diabetic Foot. IWGDF Guidelines on the prevention and management of diabetic foot disease. International Working Group on the Diabetic Foot, Maastricht, 2019.
3. National Institute of Health Diabetic Foot Consortium. Diabetic Foot Consortium, 2020.
4. International Working Group of the Diabetic Foot. Diabetic Foot-Epidemiology, Psychosocial, and Economic Factors. IWGoD, Maastricht, 2012.
5. CDC Diabetes Report Card. In: Services UDoHaH. Centers for Disease Control Prevention, Arlington, VA, 2017.
6. Dayya D, O'Neill OJ, Huedo-Medina TB, Habib N, Moore J and Iyer K: Debridement of Diabetic Foot Ulcers. Adv Wound Care (New Rochelle) 11: 666-686, 2022.
7. Baronski S and Ayello EA: Wound Care Essentials Principles and Practice. Wilkins LW, ed. Philadelphia, Wolters Kluwer, 2008.
8. den Dekker A, Davis FM, Kunkel SL and Gallagher KA: Targeting epigenetic mechanisms in diabetic wound healing. Transl Res 204: 39-50, 2019.
9. Wilkinson HN and Hardman MJ: Wound healing: Cellular mechanisms and pathological outcomes. Open Biol 10: 200223, 2020.
10. Geng K, Ma X, Jiang Z, Huang W, Gao C, Pu Y, Luo L, Xu Y and Xu Y: Innate immunity in diabetic wound healing: Focus on the mastermind hidden in chronic inflammatory. Front Pharmacol 12: 653940, 2021.
11. Wang Y, Cao Z, Wei Q, Ma K, Hu W, Huang Q, Su J, Li H, Zhang C and Fu X: VH298-loaded extracellular vesicles released from gelatin methacryloyl hydrogel facilitate diabetic wound healing by HIF-1α-mediated enhancement of angiogenesis. Acta Biomater 147: 342-355, 2022.
12. Deptuła M, Brzezicka A, Skoniecka A, Zieliński J and Pikuła M: Adipose-derived stromal cells for nonhealing wounds: Emerging opportunities and challenges. Med Res Rev 41: 2130-2171, 2021.
13. Nalisa DL, Moneruzzaman M, Changwe GJ, Mobet Y, Li LP, Ma YJ and Jiang HW: Stem cell therapy for diabetic foot ulcers: Theory and practice. J Diabetes Res 2022: 6028743, 2022.
14. Li X, Xie X, Lian W, Shi R, Han S, Zhang H, Lu L and Li M: Exosomes from adipose-derived stem cells overexpressing Nrf2 accelerate cutaneous wound healing by promoting vascularization in a diabetic foot ulcer rat model. Exp Mol Med 50: 1-14, 2018.
15. Lv Q, Deng J, Chen Y, Wang Y, Liu B and Liu J: Engineered human adipose stem-cell-derived exosomes loaded with miR-21-5p to promote diabetic cutaneous wound healing. Mol Pharm 17: 1723-1733, 2020.
16. An Y, Lin S, Tan X, Zhu S, Nie F, Zhen Y, Gu L, Zhang C, Wang B, Wei W, *et al*: Exosomes from adipose-derived stem cells and application to skin wound healing. Cell Prolif 54: e12993, 2021.
17. Wang J, Wu H, Peng Y, Zhao Y, Qin Y, Zhang Y and Xiao Z: Hypoxia adipose stem cell-derived exosomes promote high-quality healing of diabetic wound involves activation of PI3K/Akt pathways. J Nanobiotechnology 19: 202, 2021.
18. Luo H, Wang Y, Su Y, Liu D, Xiao H, Wu M, Zhao Y and Xue F: Paracrine effects of adipose-derived stem cells in cutaneous wound healing in streptozotocin-induced diabetic rats. J Wound Care 31 (Suppl 3): S29-S38, 2022.
19. Zhou C, Zhang B, Yang Y, Jiang Q, Li T, Gong J, Tang H and Zhang Q: Stem cell-derived exosomes: Emerging therapeutic opportunities for wound healing. Stem Cell Res Ther 14: 107, 2023.
20. Rezaie J, Feghhi M and Etemadi T: A review on exosomes application in clinical trials: Perspective, questions, and challenges. Cell Commun Signal 20: 145, 2022.
21. Poolman RW, Agoritsas T, Siemieniuk RA, Harris IA, Schipper IB, Mollon B, Smith M, Albin A, Nador S, Sasges W, *et al*: Low intensity pulsed ultrasound (LIPUS) for bone healing: A clinical practice guideline. BMJ 356: j576, 2017.
22. Elmajee M, Munasinghe C, Nasser AAH, Nagappa S and Mahmood A: The perceptions of clinicians using low-intensity pulsed ultrasound (LIPUS) for orthopaedic pathology: A national qualitative study. Injury 53: 3214-3219, 2022.
23. Lai WC, Iglesias BC, Mark BJ and Wang D: Low-intensity pulsed ultrasound augments tendon, Ligament, and bone-soft tissue healing in preclinical animal models: A systematic review. Arthroscopy 37: 2318-2333, 2021.
24. Sabbagh A, Beccaria K, Ling X, Marisetty A, Ott M, Caruso H, Barton E, Kong LY, Fang D, Latha K, *et al*: Opening of the blood-brain barrier using low-intensity pulsed utrasound enhances responses to immunotherapy in preclinical glioma models. Clin Cancer Res 27: 4325-4337, 2021.
25. Truong TT, Chiu WT, Lai YS, Huang H, Jiang X and Huang CC: Ca2+ signaling-mediated low-intensity pulsed ultrasound-induced proliferation and activation of motor neuron cells. Ultrasonics 124: 106739, 2022.
26. Wu Y, Gao Q, Zhu S, Wu Q, Zhu R, Zhong H, Xing C, Qu H, Wang D, Li B, *et al*: Low-intensity pulsed ultrasound regulates proliferation and differentiation of neural stem cells through notch signaling pathway. Biochem Biophys Res Commun 526: 793-798, 2020.
27. Wang X, Lin Q, Zhang T, Wang X, Cheng K, Gao M, Xia P and Li X: Low-intensity pulsed ultrasound promotes chondrogenesis of mesenchymal stem cells via regulation of autophagy. Stem Cell Res Ther 10: 41, 2019.
28. Bunnell BA, Flaat M, Gagliardi C, Patel B and Ripoll C: Adipose-derived stem cells: Isolation, expansion and differentiation. Methods 45: 115-120, 2008.
29. Hsu HH, Wang AYL, Loh CYY, Pai AA and Kao HK: Therapeutic potential of exosomes derived from diabetic adipose stem cells in cutaneous wound healing of db/db mice. Pharmaceutics 14: 1206, 2022.
30. Foster DS, Januszyk M, Yost KE, Chinta MS, Gulati GS, Nguyen AT, Burcham AR, Salhotra A, Ransom RC, Henn D, *et al*: Integrated spatial multiomics reveals fibroblast fate during tissue repair. Proc Natl Acad Sci USA 118: e2110025118, 2021.
31. Geng X, Qi Y, Liu X, Shi Y, Li H and Zhao L: A multifunctional antibacterial and self-healing hydrogel laden with bone marrow mesenchymal stem cell-derived exosomes for accelerating diabetic wound healing. Biomater Adv 133: 112613, 2022.
32. Hu Y, Tao R, Chen L, Xiong Y, Xue H, Hu L, Yan C, Xie X, Lin Z, Panayi AC, *et al*: Exosomes derived from pioglitazone-pretreated MSCs accelerate diabetic wound healing through enhancing angiogenesis. J Nanobiotechnology 19: 150, 2021.

33. Yan C, Xv Y, Lin Z, Endo Y, Xue H, Hu Y, Hu L, Chen L, Cao F, Zhou W, *et al*: Human umbilical cord mesenchymal stem cell-derived exosomes accelerate diabetic wound healing via ameliorating oxidative stress and promoting angiogenesis. Front Bioeng Biotechnol 10: 829868, 2022.
34. Pomatto M, Gai C, Negro F, Cedrino M, Grange C, Ceccotti E, Togliatto G, Collino F, Tapparo M, Figliolini F, *et al*: Differential therapeutic effect of extracellular vesicles derived by bone marrow and adipose mesenchymal stem cells on wound healing of diabetic ulcers and correlation to their cargoes. Int J Mol Sci 22: 3851, 2021.
35. Xia P, Shi Y, Wang X and Li X: Advances in the application of low-intensity pulsed ultrasound to mesenchymal stem cells. Stem Cell Res Ther 13: 214, 2022.
36. Lucchetti D, Perelli L, Colella F, Ricciardi-Tenore C, Scoarughi GL, Barbato G, Boninsegna A, De Maria R and Sgambato A: Low-intensity pulsed ultrasound affects growth, differentiation, migration, and epithelial-to-mesenchymal transition of colorectal cancer cells. J Cell Physiol 235: 5363-5377, 2020.
37. Huang D, Gao Y, Wang S, Zhang W, Cao H, Zheng L, Chen Y, Zhang S and Chen J: Impact of low-intensity pulsed ultrasound on transcription and metabolite compositions in proliferation and functionalization of human adipose-derived mesenchymal stromal cells. Sci Rep 10: 13690, 2020.
38. Cao Y, Gong Y, Liu L, Zhou Y, Fang X, Zhang C, Li Y and Li J: The use of human umbilical vein endothelial cells (HUVECs) as an in vitro model to assess the toxicity of nanoparticles to endothelium: A review. J Appl Toxicol 37: 1359-1369, 2017.
39. Cheng M, Li F, Han T, Yu ACH and Qin P: Effects of ultrasound pulse parameters on cavitation properties of flowing microbubbles under physiologically relevant conditions. Ultrason Sonochem 52: 512-521, 2019.
40. Atherton P, Lausecker F, Harrison A and Ballestrem C: Low-intensity pulsed ultrasound promotes cell motility through vinculin-controlled Rac1 GTPase activity. J Cell Sci 130: 2277-2291, 2017.
41. Jiang X, Savchenko O, Li Y, Qi S, Yang T, Zhang W and Chen J: A Review of Low-Intensity Pulsed Ultrasound for Therapeutic Applications. IEEE Trans Biomed Eng 66: 2704-2718, 2019.
42. Harrison A and Alt V: Low-intensity pulsed ultrasound (LIPUS) for stimulation of bone healing-A narrative review. Injury 52 (Suppl): S91-S96, 2021.
43. Razavi M, Zheng F, Telichko A, Ullah M, Dahl J and Thakor AS: Effect of pulsed focused ultrasound on the native pancreas. Ultrasound Med Biol 46: 630-638, 2019.
44. Burks SR, Ziadloo A, Hancock HA, Chaudhry A, Dean DD, Lewis BK, Frenkel V and Frank JA: Investigation of cellular and molecular responses to pulsed focused ultrasound in a mouse model. PLoS One 6: e24730, 2011.
45. Yoon CW, Jung H, Goo K, Moon S, Koo KM, Lee NS, Weitz AC and Shung KK: Low-intensity ultrasound modulates Ca2+ dynamics in human mesenchymal stem cells via connexin 43 hemichannel. Ann Biomed Eng 46: 48-59, 2018.
46. King AJ: The use of animal models in diabetes research. Br J Pharmacol 166: 877-894, 2012.